



Synthesis and evaluation of 1-(4-[¹⁸F]fluoroethyl)-7-(4'-methyl)curcumin with improved brain permeability for β -amyloid plaque imaging

Iljung Lee^a, Jehoon Yang^b, Jung Hee Lee^b, Yearn Seong Choe^{a,*}

^a Department of Nuclear Medicine, Samsung Medical Center, Sungkyunkwan University School of Medicine, Seoul, South Korea

^b Department of Radiology, Samsung Medical Center, Sungkyunkwan University School of Medicine, Seoul, South Korea

ARTICLE INFO

Article history:

Received 29 June 2011

Revised 21 July 2011

Accepted 1 August 2011

Available online 10 August 2011

Keywords:

Alzheimer's disease

β -Amyloid plaques

1-(4-[¹⁸F]fluoroethyl)-7-(4'-

methyl)curcumin

Brain permeability

ABSTRACT

Alzheimer's disease is characterized by the accumulation of β -amyloid ($A\beta$) plaques and neurofibrillary tangles (NFTs) in the brain. We previously developed [¹⁸F]fluoropropylcurcumin ([¹⁸F]FP-curcumin), which demonstrated excellent binding affinity ($K_i = 0.07$ nM) for $A\beta(1-40)$ aggregates and good pharmacokinetics in normal mouse brains. However, its initial brain uptake was poor (0.52% ID/g at 2 min post-injection). Therefore, in the present study, fluorine-substituted 4,4'-bissubstituted or pegylated curcumin derivatives were synthesized and evaluated. Their binding affinities for $A\beta(1-42)$ aggregates were measured and 1-(4-fluoroethyl)-7-(4'-methyl)curcumin (**1**) had the highest binding affinity ($K_i = 2.12$ nM). Fluorescence staining of Tg APP/PS-1 mouse brain sections demonstrated high and specific labeling of $A\beta$ plaques by **1** in the cortex region, which was confirmed with thioflavin-S staining of the same spots in the adjacent brain sections. Radioligand [¹⁸F]**1** was found to have an appropriate partition coefficient ($\log P_{o/w} = 2.40$), and its tissue distribution in normal mice demonstrated improved brain permeability (1.44% ID/g at 2 min post-injection) compared to that of [¹⁸F]FP-curcumin by a factor of 2.8 and fast wash-out from mouse brains (0.45% ID/g at 30 min post-injection). These results suggest that [¹⁸F]**1** may hold promise as a PET radioligand for $A\beta$ plaque imaging.

© 2011 Elsevier Ltd. All rights reserved.

Alzheimer's disease (AD) is characterized by the accumulation of β -amyloid ($A\beta$) plaques and neurofibrillary tangles (NFTs) in the brain.¹⁻³ Although the causes of AD are still unknown, it is the general consensus that $A\beta$ plaques and NFTs may play a major role in the development of the disease. Therefore, in vivo imaging of $A\beta$ plaques and/or NFTs may be beneficial for the diagnosis, staging, and treatment of AD.

Most radioligands used for $A\beta$ plaque imaging are derived from highly conjugated fluorescent dyes, such as Congo red (CR), Chrysin G (CG), or thioflavin-T (Fig. 1), which have been used for fluorescent staining of $A\beta$ plaques and NFTs in postmortem AD brain sections.⁴⁻⁶ A neutral benzothiazole derivative, [¹¹C]6-OH-BTA-1 (PIB, $K_i = 0.87$ nM), is the most well characterized radioligand, demonstrating minimal retention in the subcortical white matter of AD patients compared to other benzothiazole-based radioligands.⁷⁻¹³ Another ¹¹C-labeled radioligand, 2-(6-([¹¹C]methylamino)pyridin-3-yl)benzo[d]thiazol-6-ol (AZD2184, $K_i = 1.70$ nM), is also a promising $A\beta$ plaque imaging agent because [³H]AZD2184 demonstrated a higher pre-frontal cortex to subcortical white matter uptake ratio compared to [³H]PIB in cortical brain sections from transgenic mice and AD patients.¹⁴ However, the short half-life (20 min) of ¹¹C may limit its usefulness in

widespread clinical application. As an alternative, ¹⁸F-labeled ligands with longer half-lives may be beneficial for clinical use; some of these are currently undergoing clinical trials or have been conditionally approved by the FDA: a PIB derivative, 2-(3-[¹⁸F]fluoro-4-(methylamino)phenyl)benzo[d]thiazol-6-ol ([¹⁸F]flutemetamol, 3'-[¹⁸F]F-PIB, GE067),¹⁵⁻¹⁷ and pegylated stilbene and styrylpyridine derivatives, {4-[2-(4-{2-[2-(2-[¹⁸F]fluoro-ethoxy)-ethoxy]-ethoxy)-phenyl]-vinyl]-phenyl}-methyl-amine ([¹⁸F]florbetaben, BAY 94-9172)^{18,19} and (E)-4-(2-(6-(2-(2-(2-[¹⁸F]fluoroethoxy)ethoxy)ethoxy)pyridin-3-yl)vinyl)-N-methylaniline ([¹⁸F]florbetapir, AV-45) (Fig. 1).^{20,21} Preliminary results demonstrated that these ¹⁸F-labeled ligands are potentially useful for PET imaging of $A\beta$ plaques in AD patient brains.¹⁵⁻²² However, these ¹⁸F-labeled radioligands have higher subcortical white matter uptake than ¹¹C-PIB, which may disturb distinguishing AD patients from healthy subjects.

A highly conjugated dimeric ligand, (1E,3Z,6E)-1,7-bis(4-hydroxy-3-methoxyphenyl)-3-hydroxy-hepta-1,3,6-trien-5-one (curcumin) has been extensively studied for its anticancer, antioxidant, and anti-inflammatory activities.^{23,24} It has also been found that dietary curcumin lowered the $A\beta$ plaque burden in the hippocampus and cortex regions of APPsw Tg2576 transgenic mouse brain sections and stained $A\beta$ plaques in the hippocampus regions of transgenic mouse brain sections and postmortem AD brains.^{25,26} In addition, it was recently reported that CRANAD-3, a curcumin

* Corresponding author. Tel.: +82 2 3410 2623; fax: +82 2 3410 2667.

E-mail address: ysnm.choe@samsung.com (Y.S. Choe).

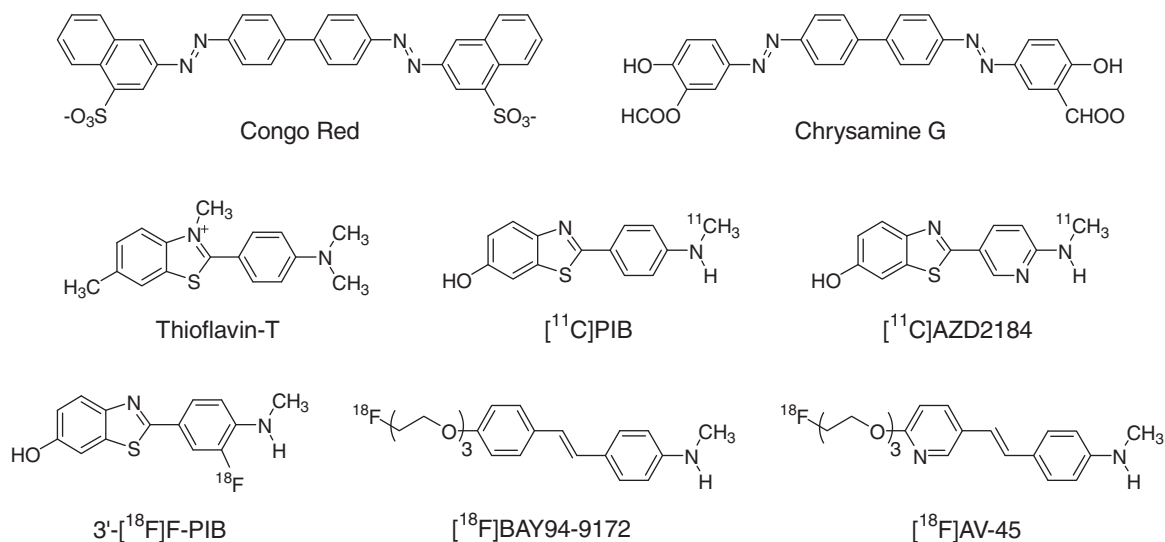


Figure 1. Chemical structures of Congo red, Chrysamine G, thioflavin-T, [¹¹C]PIB, [¹¹C]AZD2184, 3-[¹⁸F]F-PIB, [¹⁸F]BAY94-9172, and [¹⁸F]AV-45.

derivative, detects Aβ(1–42) species from monomer to plaques.²⁷ Diagnosis of AD in its early stages will be very crucial given disease-modifying drugs that are available for clinical use; detection of Aβ(1–42) species prior to plaque formation may play a key role in the early diagnosis of AD.

We previously developed a ¹⁸F-labeled curcumin derivative, (1*E*,4*Z*,6*E*)-1-(4-(3-[¹⁸F]fluoropropoxy)-3-methoxyphenyl)-5-hydroxy-7-(4-hydroxy-3-methoxyphenyl)-hepta-1,4,6-trien-3-one (fluoropropylcurcumin; FP-curcumin).²⁸ However, despite its excellent binding affinity ($K_i = 0.07$ nM) for Aβ(1–40) aggregates, its initial brain uptake was relatively low (0.52% ID/g at 2 min post-injection). This may be explained by its rapid metabolism in the liver and in the intestinal wall, like curcumin.²⁹ However, [¹⁸F]FP-curcumin has a high and specific binding to Aβ plaques once it is taken up by the brain. This is supported by reports that this radioligand showed higher hippocampus (Aβ plaque rich region) to cerebellum uptake ratio compared to that of [¹¹C]PIB (3.0–3.5 vs 1.5) in transgenic mouse (Tg2576) brain sections, and that uptake by the hippocampus was decreased by 70% in the presence of 10 μM PIB.³⁰ Thus, improving the brain permeability of curcumin-based radioligands is a key element to consider for such radioligands to be useful for Aβ plaque imaging.

In order to improve the brain permeability of curcumin derivatives, the lipophilicity was adjusted such that a *para*-OH group of a phenyl ring was substituted with an alkoxy group or a polyethoxy

group. Synthetic pathways of curcumin derivatives, **1–5** (Fig. 2), are shown in Schemes 1 and 2. The curcumin derivatives were synthesized by aldol condensation of (1*E*,4*Z*)-5-hydroxy-1-phenylhexa-1,4-dien-3-one compound (**6** or **7**) and the corresponding vanillin derivatives, **8**, **9**, **15**, or **16**. In this reaction, the 1,3-diketone of the **6** or **7**-boron complex was formed, which was then reacted with aldehyde **8**, **9**, **15**, or **16** in the presence of amine. Dilute acid treatment of the boron complex yielded curcumin derivatives **1–5** (Scheme 1). Compounds **8–12** were prepared in 57–88% yields from vanillin and the corresponding fluoroalkyl tosylate, 2-bromoethanol, 2-(2-chloroethoxy)ethanol, or 2-(2-(2-chloroethoxy)ethoxy)ethanol in the presence of K₂CO₃ (Scheme 2). Fluoropegylated vanillin derivatives, **15** and **16**, were prepared from fluorination of the corresponding methanesulfonyl compounds, **13** and **14**, with CsF (Scheme 2). Compounds **13** and **14** were prepared from methanesulfonylation of **11** and **12**. The nosylate precursor (**19**) for synthesis of [¹⁸F]**1** was synthesized from **18** using 4-nitrobenzenesulfonyl chloride and Et₃N in the presence of B₂O₃ (Schemes 2 and 3). Compound **18** was synthesized from aldol condensation of either **17** and 3,4-dimethylbenzaldehyde or **7** and **10** (Schemes 1 and 2). The former method was used because the residual vanillin derivative (**10**) remained in the product based on ¹H NMR analysis in the latter method. Compound **17** was prepared by aldol condensation of **10** and 2,4-pentanedione in the presence of B₂O₃, (*n*-BuO)B, and *n*-butylamine and then purified

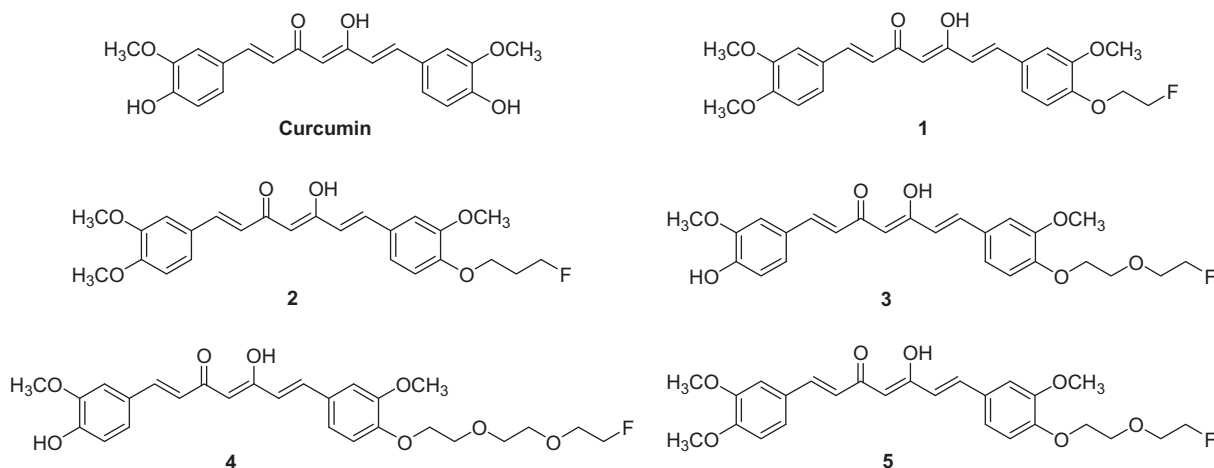
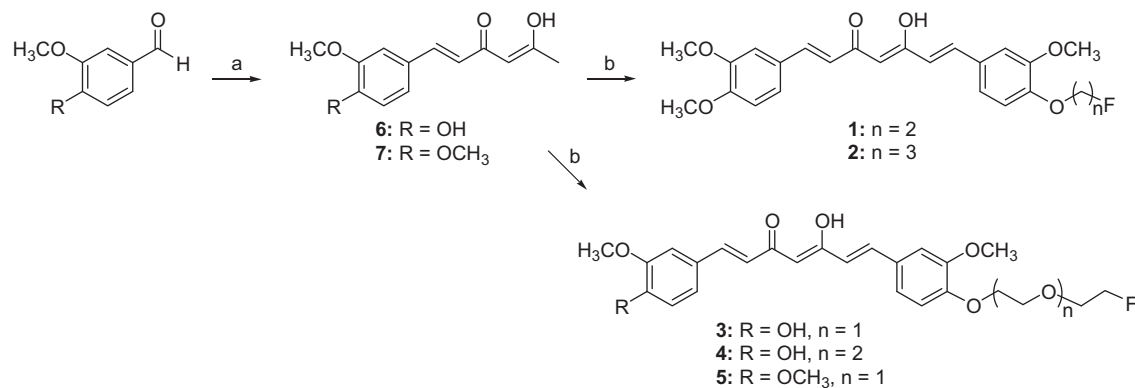
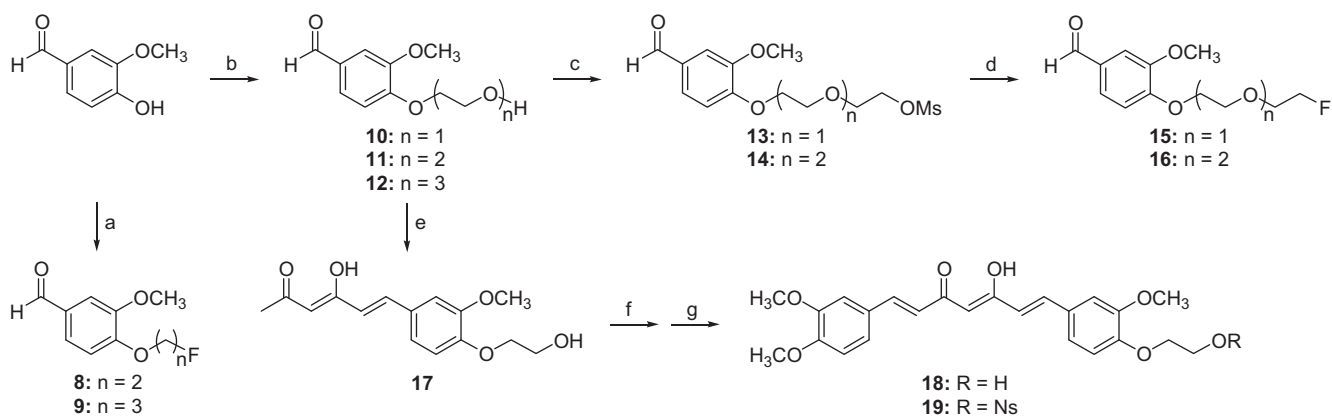


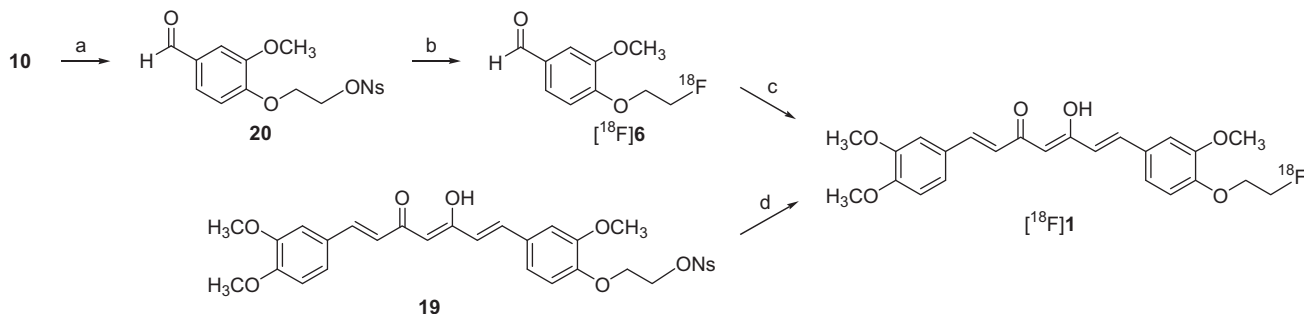
Figure 2. Chemical structures of curcumin and fluorine-substituted curcumin derivatives.



Scheme 1. Reagents and conditions: (a) 2,4-pentanedione, B₂O₃, ethyl acetate, (*n*-BuO)₃B, *n*-BuNH₂, 100 °C, 1 h, 1 N HCl, 50 °C, 30 min; (b) vanillin derivative (**8**, **9**, **15**, or **16**), B₂O₃, ethyl acetate, (*n*-BuO)₃B, piperidine, 80 °C, 30 min, 0.4 N HCl, 50 °C, 30 min.



Scheme 2. Reagents and conditions: (a) fluoroalkyl tosylate, K₂CO₃, CH₃CN, 110 °C, 1.5 h; (b) 2-bromoethanol, 2-(2-chloroethoxy)ethanol, or 2-(2-(2-chloroethoxy)ethoxy)ethanol, DMF, 100 °C, 5 h; (c) MsCl, Et₃N, CH₂Cl₂, room temperature, 3 h; (d) CsF, CH₃CN, 100 °C, 17 h; (e) 2,4-pentanedione, B₂O₃, ethyl acetate, (*n*-BuO)₃B, *n*-butylamine, 100 °C, 1 h, 1 N HCl, 50 °C, 30 min; (f) 3,4-dimethylbenzaldehyde, B₂O₃, ethyl acetate, (*n*-BuO)₃B, piperidine, 80 °C, 30 min, 0.4 N HCl, 50 °C, 30 min; (g) B₂O₃, CH₂Cl₂, Et₃N, NsCl, room temperature, 5 h, 0.4 N HCl, 50 °C, 30 min.



Scheme 3. Reagents and conditions: (a) Et₃N, NsCl, CH₂Cl₂, room temperature, 1 h; (b) *n*-Bu₄N[¹⁸F]F, CH₃CN, 120 °C, 15 min; (c) **7**, B₂O₃, (*n*-BuO)₃B, piperidine, ethyl acetate, 120 °C, 20 min, 0.4 N HCl, 90 °C, 5 min; (d) *n*-Bu₄N[¹⁸F]F, THF, 95 °C, 20 min.

by flash column chromatography followed by recrystallization from ethanol (Scheme 2). Without the recrystallization step, **10** remained in the product based on ¹H NMR analysis.

The binding affinity of curcumin derivatives, **1–5** was determined using Aβ(1–42) aggregates and [¹²⁵I]MSB, and non-specific binding was measured in the presence of 10 μM Chrysamine G (CG). The K_d value of [¹²⁵I]MSB for binding to Aβ(1–42) aggregates was 1.19 nM, similar to the reported value of 0.73 nM.¹⁹ The K_i value of CG (0.43 nM) was also comparable to the reported value

(0.4 nM).¹⁹ K_i values of fluorine-substituted curcumin derivatives were desirable, ranging from 2.12 to 4.65 nM (Table 1). Of the derivatives, **1** exhibited the highest binding affinity (K_i = 2.12 nM). Binding affinity was slightly decreased by pegylation (K_i = 3.01–4.65 nM), and 7-(4'-methyl) derivative **5** showed a higher binding affinity (3.01 nM) than unmethylated derivatives **3** and **4**, suggesting that hydroxyl groups on phenyl rings are not required for avid binding to Aβ(1–42) aggregates. This result indicated that **1** had similar binding affinity to those of the radiopharmaceuticals

Table 1
 K_i (nM) of ligands for A β (1–42) aggregates

Ligand	K_i (nM)
Chrysamine G	0.43 \pm 0.068
Curcumin	3.57 \pm 0.025
1	2.12 \pm 0.097
2	2.69 \pm 0.033
3	4.65 \pm 0.267
4	4.44 \pm 0.313
5	3.01 \pm 0.087

Values are means \pm SD ($n = 3$).

currently under clinical development (0.74–2.87 nM), although the assays were done against A β (1–42) aggregates in the former and AD brain homogenates in the latter.^{18,21,22}

Therefore, **1** was chosen for radiolabeling with ¹⁸F and further evaluation as an A β plaque imaging agent for PET, because of its high binding affinity for A β (1–42) aggregates and appropriate lipophilicity based on TLC analysis. Pegylated compounds **3–5** were found to be more polar than FP-curcumin ($\log P_{o/w} = 1.84$) by TLC, which may result in poor initial brain uptake. Radioligand [¹⁸F]**1** was synthesized as shown in Scheme 3. The synthesis was carried out using two methods: one-step and two-step radiolabeling. The former was carried out by ¹⁸F-labeling of the nosylate precursor (**19**); the decay-corrected radiochemical yield was 10–17% and total synthesis time was 60 min. Although [¹⁸F]**1** was also synthesized from **19** with *n*-Bu₄N[¹⁸F]F in the presence of B₂O₃, the decay-corrected radiochemical yield was in the same range with the reaction performed in the absence of B₂O₃. However, the two-step reaction using aldol condensation of [¹⁸F]**6** and **7** gave [¹⁸F]**1** in 15–25% yield and with higher specific activity. The use of tosylate precursor in place of the nosylate precursor (**19**) afforded [¹⁸F]**1** in a 5–10% yield with lower specific activity. Therefore, the two-step method was used in this study. The radiochemical yield of [¹⁸F]**6** from **20** and *n*-Bu₄N[¹⁸F]F based on TLC analysis was 70% or greater. The subsequent aldol condensation of [¹⁸F]**6** and **7** in the presence of B₂O₃, (*n*-BuO)₃B, and piperidine followed by HPLC purification gave the product a decay-corrected overall radiochemical yield of 15–25% and a specific activity of 37.6 GBq/ μ mol. The total synthesis time including HPLC purification was 90–100 min. The partition coefficient of [¹⁸F]**1** ($\log P_{o/w} = 2.4$) was found to be higher than that of [¹⁸F]FP-curcumin ($\log P_{o/w} = 1.84$).²⁸

Curcumin has strong fluorescence based on its highly conjugated structure. To confirm whether **1** could label A β plaques

Table 2
Tissue distribution of [¹⁸F]**1** in normal mice

Organ	% ID/g			
	2 min	30 min	60 min	120 min
Blood	9.76 \pm 0.59	1.26 \pm 0.08	0.89 \pm 0.15	0.67 \pm 0.13
Heart	7.18 \pm 0.58	1.68 \pm 0.33	1.30 \pm 0.19	1.54 \pm 0.45
Lung	23.78 \pm 2.92	3.94 \pm 0.64	2.27 \pm 0.56	2.19 \pm 0.46
Liver	38.83 \pm 2.88	43.02 \pm 3.33	26.83 \pm 0.43	12.51 \pm 1.45
Spleen	16.41 \pm 2.92	20.80 \pm 12.3	10.59 \pm 1.25	8.08 \pm 1.90
Kidney	10.95 \pm 0.58	4.01 \pm 1.24	2.25 \pm 0.90	1.42 \pm 0.15
Muscle	0.89 \pm 0.34	0.76 \pm 0.29	0.47 \pm 0.05	0.37 \pm 0.07
Femur	1.86 \pm 0.13	1.08 \pm 0.08	1.00 \pm 0.16	1.62 \pm 0.12
Brain	1.44 \pm 0.09	0.45 \pm 0.04	0.43 \pm 0.05	0.29 \pm 0.03

Values are means \pm SD ($n = 4$).

in vivo, fluorescence staining of plaques by **1** and thioflavin-S were compared using the brain sections from both a double transgenic mouse (Tg APP/PS-1) and a wild-type mouse (Fig. 3). Many plaques in the cortex region of the transgenic mouse brain were stained with **1** (Fig. 3A and E), and the fluorescence staining pattern was consistent with that observed with thioflavin-S, a dye used for staining A β plaques in vitro (Fig. 3B and F). In contrast, there were no notable plaques stained with either **1** or thioflavin-S in wild-type mouse brain sections (Fig. 3C–H). This result suggests that ligand **1** distinctively stains A β plaques in transgenic mouse brains.

In order to investigate the in vivo pharmacokinetics of [¹⁸F]**1**, tissue distribution in normal mice was performed. High radioactivity was accumulated in the lung, liver, and spleen at 2 min post-injection and decreased over time. Brain uptake of [¹⁸F]**1** was 1.44% ID/g at 2 min post-injection and was rapidly washed out from the brain (2-min to 60-min uptake ratio, 3.35) (Table 2). The initial brain uptake was improved compared to that of [¹⁸F]FP-curcumin by a factor of 2.8,²⁴ probably because of the increased lipophilicity. This is a notable improvement in brain permeability, considering unique properties of curcumin derivatives. In addition, [¹⁸F]**1** did not appear to undergo metabolic defluorination due to a constant level of femur uptake with time (1.00–1.86% ID/g). These results indicated that [¹⁸F]**1** had favorable pharmacokinetics in normal mouse brains. The recent studies demonstrated that the radiopharmaceuticals currently under clinical development (BAY 94-9172, and AV-45) had high initial brain uptake (7.33–7.77% ID/g) in normal mice and fast wash-out from mouse brains (2-min to 60-min uptake ratios, 3.90–4.82).^{18,21} However, further studies with ¹⁸F-labeled curcumin-based ligands are clearly warranted if their brain permeability could be improved, because they

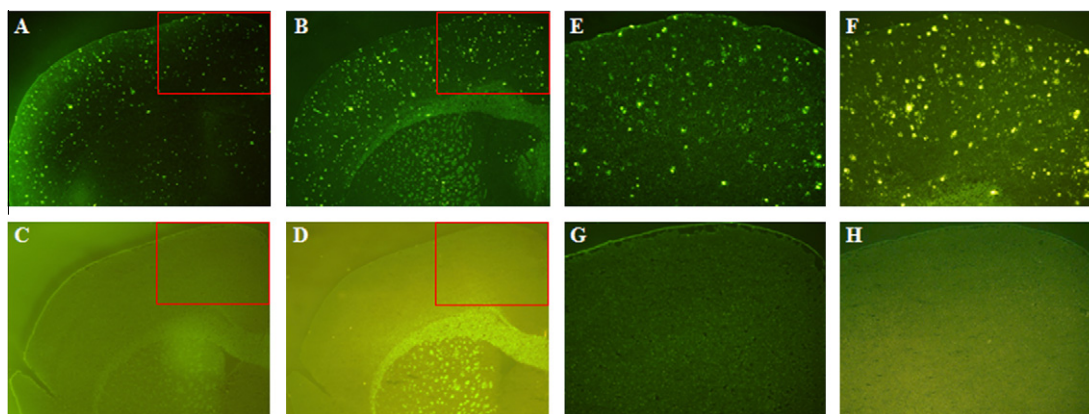


Figure 3. (Left) A double transgenic mouse brain section stained with **1** ($\times 40$) (A), the adjacent section stained with thioflavin-S ($\times 40$) (B), an age-matched wild-type mouse brain section stained with **1** ($\times 40$) (C), and the adjacent section stained with thioflavin-S ($\times 40$) (D). (Right) Magnification of the cortex regions in red boxes of left panels ($\times 100$). A double transgenic mouse brain section stained with **1** (E), the adjacent section stained with thioflavin-S (F), an age-matched wild-type mouse brain section stained with **1** (G), and the adjacent section stained with thioflavin-S (H).

have different in vivo binding sites from thioflavin-T based radioligands for A β plaques and thus may have different in vivo properties, such as low subcortical white matter uptake or detection of A β (1–42) species prior to plaque formation.

In conclusion, five curcumin derivatives were synthesized and evaluated in vitro and in vivo. Of the derivatives, [¹⁸F]1 demonstrated a high binding affinity for A β (1–42) aggregates, suitable lipophilicity, specific binding to A β plaques in Tg APP/PS-1 mouse brain sections, improved brain permeability compared to that of [¹⁸F]FP-curcumin, and fast wash-out from normal mouse brains. These results suggest that [¹⁸F]1 may be a potential radioligand for A β plaque imaging.

Acknowledgments

This study was supported in part by the Samsung Biomedical Research Institute grant (C-A6-228-3) and by the Nuclear Research Development Program of the Korea Science and Engineering Foundation (KOSEF) grant funded by the Korean government (MEST) (Grant code: 2010-0018315).

Supplementary data

Supplementary data associated with this article can be found, in the online version, at doi:10.1016/j.bmcl.2011.08.003.

References and notes

- Ginsberg, S. D.; Schmidt, M. L.; Crino, P. B.; Eberwine, J. H.; Lee, V. M. Y.; Trojanowski, J. Q. *Cerebral Cortex: Neurodegenerative Age-related Changes in Structure Function of Cerebral Cortex* In Peters, A., Morrison, J. H., Eds.; Kluwer Academic/Plenum Publishers: New York, 1999; pp 603–654.
- Lee, V. M.; Trojanowski, J. Q. *Neuron* **1999**, *24*, 507.
- Selkoe, D. J. *JAMA* **2000**, *283*, 1615.
- Mathis, C. A.; Wang, Y.; Klunk, W. E. *Curr. Pharm. Design* **2004**, *10*, 1469.
- Ashburn, T. T.; Han, H.; McGuinness, B. F.; Lansbury, P. T., Jr. *Chem. Biol.* **1996**, *3*, 351.
- Klunk, W. E.; Pettegrew, J. W.; Abraham, D. J. *J. Histochem. Cytochem.* **1989**, *37*, 1273.
- Mathis, C. A.; Mahmood, K.; Debnath, M. L.; Klunk, W. E. *J. Labelled Compd. Radiopharm.* **1997**, *39*, 594.
- Klunk, W. E.; Wang, Y.; Huang, G.; Debnath, M. L.; Holt, D. P.; Mathis, C. A. *Life Sci.* **2001**, *69*, 1471.
- Mathis, C. A.; Bacskai, B. J.; Kajdasz, S. T.; McLellan, M. E.; Frosch, M. P.; Hyman, B. T.; Holt, D. P.; Wang, Y.; Huang, G. F.; Debnath, M. L.; Klunk, W. E. *Bioorg. Med. Chem. Lett.* **2002**, *12*, 295.
- Mathis, C. A.; Wang, Y.; Holt, D. P.; Huang, G. F.; Debnath, M. L.; Klunk, W. E. *J. Med. Chem.* **2003**, *46*, 2740.
- Klunk, W. E.; Engler, H.; Nordberg, A.; Wang, Y.; Blomqvist, G.; Holt, D. P.; Bergström, M.; Savitcheva, I.; Huang, G.; Estrada, S.; Ausén, B.; Debnath, M. L.; Barletta, J.; Price, J. C.; Sandell, J.; Lopresti, B. J.; Wall, A.; Koivisto, P.; Antoni, G.; Mathis, C. A.; Långström, B. *Ann. Neurol.* **2004**, *55*, 306.
- Lopresti, B. J.; Klunk, W. E.; Mathis, C. A.; Hoge, J. A.; Ziolkowski, S. K.; Lu, X.; Meltzer, C. C.; Schimmel, K.; Tsopelas, N. D.; DeKosky, S. T.; Price, J. C. *J. Nucl. Med.* **2005**, *46*, 1959.
- Rowe, C. C.; Ackermann, U.; Gong, S. J.; Pike, K.; Savage, G.; Cowie, T. F.; Dickinson, K. L.; Maruff, P.; Darby, D.; Smith, C.; Woodward, M.; Merory, J.; Tochon-Danguy, H.; O'Keefe, G.; Klunk, W. E.; Mathis, C. A.; Price, J. C.; Masters, C. L.; Villemagne, V. L. *Neurology* **2007**, *68*, 1718.
- Johnson, A. E.; Jeppsson, F.; Sandell, J.; Wensbo, D.; Neelissen, J. A. M.; Juréus, A.; Ström, P.; Norman, H.; Farde, L.; Svensson, S. P. *S. J. Neurochem.* **2009**, *108*, 1177.
- Mathis, C. A.; Ikonomic, M. D.; Debnath, M. L.; Hamilton, R. L.; DeKosky, S. T.; Klunk, W. E. *Neuroimage* **2008**, *41*, T113.
- Koole, M.; Lewis, D. M.; Buckley, C.; Nelissen, N.; Vandenbulcke, M.; Brooks, D. J.; Bandenbeghe, R.; Van Laere, K. *J. Nucl. Med.* **2009**, *50*, 818.
- Nelissen, N.; Laere, K. V.; Thurfjell, L.; Owenius, R.; Vandenbulcke, M.; Koole, M.; Bormans, G.; Brooks, D. J.; Vandenbergh, R. *J. Nucl. Med.* **2009**, *50*, 1251.
- Zhang, W.; Oya, S.; Kung, M. P.; Hou, C.; Marier, D. L.; Kung, H. F. *Nucl. Med. Biol.* **2005**, *32*, 799.
- Rowe, C. C.; Ackerman, U.; Browne, W.; Mulligan, R.; Pike, K. L.; O'Keefe, G.; Tochon-Danguy, H.; Chan, G.; Berlangieri, S. U.; Jones, G.; Dickinson-Rowe, K. L.; Kung, H. F.; Zhang, W.; Kung, M. P.; Skovronsky, D.; Dyrks, T.; Holl, G.; Krause, S.; Friebe, M.; Lehman, L.; Lindemann, S.; Dinkelborg, L. M.; Masters, C. L.; Villemagne, V. L. *Lancet Neurol.* **2008**, *7*, 129.
- Zhang, W.; Kung, M. P.; Oya, S.; Hou, C.; Kung, H. F. *Nucl. Med. Biol.* **2007**, *34*, 89.
- Choi, S. R.; Golding, G.; Zhuang, Z.; Zhang, W.; Lim, N.; Hefti, F.; Benedum, T. E.; Kilbourn, M. R.; Skovronsky, D.; Kung, H. F. *J. Nucl. Med.* **2009**, *50*, 1887.
- Kung, H. F.; Choi, S. R.; Qu, W.; Zhang, W.; Skovronsky, D. *J. Med. Chem.* **2010**, *53*, 933.
- Cheng, A. L.; Hsu, C. H.; Lin, J. K.; Hsu, M. M.; Ho, Y. F.; Shen, T. S.; Ko, J. Y.; Lin, J. T.; Lin, B. R.; Ming-Shiang, W.; Yu, H. S.; Jee, S. H.; Chen, G. S.; Chen, T. M.; Chen, C. A.; Lai, M. K.; Pu, Y. S.; Pan, M. H.; Wang, Y. J.; Tsai, C. C.; Hsieh, C. Y. *Anticancer Res.* **2001**, *21*, 2895.
- Lin, J. K.; Shih, C. A. *Carcinogenesis* **1994**, *15*, 1717.
- Lim, G. P.; Chu, T.; Yang, F.; Beech, W.; Frautschy, S. A.; Cole, G. M. *J. Neurosci.* **2001**, *21*, 8370.
- Yang, F.; Lim, G. P.; Befum, A. N.; Ubeda, O. J.; Simmons, M. R.; Ambegaokar, S. S.; Chen, P.; Kaye, R.; Glabe, C. G.; Frautschy, S. A.; Cole, G. M. *J. Biol. Chem.* **2005**, *280*, 5892.
- Ran, C.; Moore, A. World Molecular Imaging Congress. Kyoto, Japan, **2010**; Abstract.
- Ryu, E. K.; Choe, Y. S.; Lee, K. H.; Choi, Y.; Kim, B. T. *J. Med. Chem.* **2006**, *49*, 6111.
- Shoba, G.; Joy, D.; Joseph, T.; Majeed, M.; Rajendran, R.; Srinivas, P. S. *Planta Med.* **1998**, *64*, 353.
- Patel, P. C.; Sarsoza, F.; Vasilevko, V.; Pan, M. L.; Tsu, W.; Constantinescu, C.; Coleman, R.; Head, E.; Mukherjee, J. *NeuroImage* **2008**, *41S*, T115.